JOURNAL OF VIROLOGY, Dec. 1991, p. 6486–6494
0022-538X/91/126486-09$02.00/0

Vol. 65, No. 12

Interaction of a Cellular 57-Kilodalton Protein with the Internal Translation Initiation Site of Foot-and-Mouth Disease Virus

NORBERT LUZ AND EWALD BECK†*

Zentrum für Molekulare Biologie Heidelberg, University of Heidelberg, Im Neuenheimer Feld 282, D-6900 Heidelberg, Germany

Received 3 July 1991/Accepted 29 August 1991

A cellular 57-kDa protein (p57) that binds specifically to the internal translation initiation site in the 5′ untranslated region of foot-and-mouth disease virus RNA was detected in cell extracts of different mammalian species by UV cross-linking. The protein binds to two distinct sites of the translation control region which have as the only common sequence a UUUC motif. The first binding site consists of a conserved hairpin structure, whereas the second binding site contains an essential pyrimidine-rich region without obvious secondary structure. Competition experiments indicate that the complexes with the two binding sites were formed by a single p57 species. The protein binds also to the 5′ untranslated region of other picornaviruses. Results from footprint analyses with foot-and-mouth disease RNA suggest the participation of additional cellular factors in the translation initiation complex.

The positive-strand RNA genome of foot-and-mouth disease virus (FMDV), a member of the *Picornaviridae* family, includes a 5′ untranslated region (5′UTR) of approximately 1,300 nucleotides (nt). This region is presumed to contain sequence elements controlling the replication of viral RNA, packaging of RNA into capsids, and translation of the viral polyprotein. For several members of the picornavirus family, it has been shown that ribosomes initiate translation by internal entry onto the 5′UTR, without scanning from the 5′ end of the viral RNA (11, 24; for a review, see reference 10). By mutagenesis of the 5′UTR of FMDV, we have shown that a region of approximately 450 nt preceding the open reading frame of the viral polyprotein is involved in the regulation of internal translation initiation (16). Modifications in multiple sites of this control region and in particular in a pyrimidine-rich sequence preceding the start codon led to a strong decrease of the translation efficiency.

Efficient translation initiation at the authentic picornaviral start codon apparently depends on specific factors provided by the host cell. Faithful translation of poliovirus RNA in rabbit reticulocyte lysates, for example, depends on the addition of a cytoplasmic HeLa cell extract (5), and binding of cellular proteins to multiple sites of the poliovirus 5′UTR has been demonstrated (3). Moreover, cellular 50- and 52-kDa proteins have been shown to interact with specific regions of the internal ribosomal entry site (IRES) of poliovirus RNA (19, 21).

Recently, we showed that a ribosome-associated 57-kDa protein (p57) from rabbit reticulocytes was linked to the IRES of FMDV by UV cross-linking. Binding studies with different RNA fragments revealed that this protein interacts with two distinct sites of the IRES (18). Similarly, a cellular 57-kDa protein has been shown to interact with the 5′UTR of encephalomyocarditis virus (EMCV), a related picornavirus (13).

In this study, we analyzed the mode of interaction of p57 with the internal translation initiation site of FMDV in more detail, using site-directed mutagenesis of a putative binding site and RNA footprinting, and determined the affinity to different binding sites by competition experiments. In addition, we studied the interaction of p57 with the RNA of other picornaviruses and determined the occurrence of this protein in extracts from various cell types.

MATERIALS AND METHODS

Construction of plasmids. Construction of pSP65-derived plasmids pSP449, pSP450, and pSP444 containing parts of the 5′UTR of FMDV O1K has been described previously (18). Another set of pSP plasmids (pSP436Δ519-559, pSP436Δ581-672, and pSP440-1 to pSP440-29) has been described by Kühn et al. (16). Plasmids pSP439-1 to pSP439-29 were derived from pSP440-1 to pSP440-29 by deletion of the 566-bp *Hin*dIII fragment (nt 176 to 742 of FMDV [8]). Plasmid pSP3,0-3,8 was constructed by insertion of an 847-bp *Bam*HI-*Hin*dIII fragment (nt 3000 to 3847 of FMDV [8]) into pSP65. Plasmid pSP5,4-6,4 has been described by Falk et al. (6), and plasmids pS32A3 (EMCV 5′UTR) and pT7-XLmyr- (poliovirus 5′UTR) have been described by Jang et al. (12) and Kräusslich et al. (15), respectively.

In vitro transcription. In vitro transcription of linearized DNA templates (see Fig. 1A for details) with SP6 RNA polymerase was essentially performed by standard procedures (20). Labeled RNAs were derived by using 10 μM [α-^{32}P]UTP (60 Ci/mmol; Amersham Corp.). In vitro transcription of linearized plasmids pS32A3 and pT7-XLmyr- with T7 RNA polymerase was performed as described by van der Werf et al. (30). Labeled RNAs were derived by using 55 μM [α-^{32}P]UTP (40 Ci/mmol; Amersham) and separated from free nucleotides by gel filtration on Sephadex G-100 (Pharmacia).

Preparation of cell extracts. The rabbit reticulocyte lysate was prepared according to Clemens (2), and the ribosomal salt wash fraction was obtained by the method of Woodley et al. (31).

Liver tissue from rats was extracted according to the method of Dissous et al. (4) in a buffer described by Nygård

* Corresponding author.
† Present address: Biochemisches Institut der Justus-Liebig-Universität–Molekularbiologie, Friedrichstrasse 24, D-6300 Giessen, Germany.

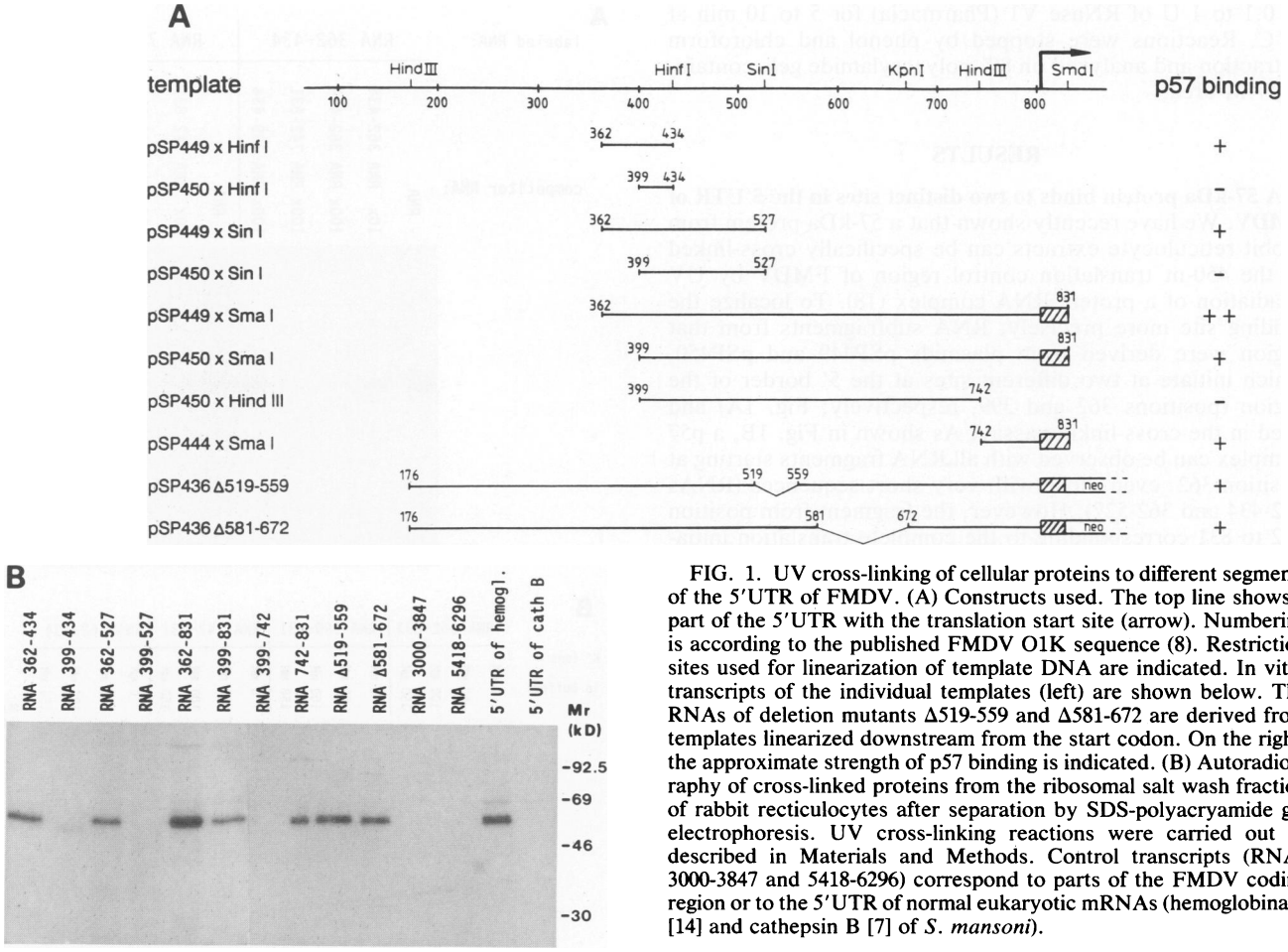

FIG. 1. UV cross-linking of cellular proteins to different segments of the 5'UTR of FMDV. (A) Constructs used. The top line shows a part of the 5'UTR with the translation start site (arrow). Numbering is according to the published FMDV O1K sequence (8). Restriction sites used for linearization of template DNA are indicated. In vitro transcripts of the individual templates (left) are shown below. The RNAs of deletion mutants Δ519-559 and Δ581-672 are derived from templates linearized downstream from the start codon. On the right, the approximate strength of p57 binding is indicated. (B) Autoradiography of cross-linked proteins from the ribosomal salt wash fraction of rabbit recticulocytes after separation by SDS-polyacryamide gel electrophoresis. UV cross-linking reactions were carried out as described in Materials and Methods. Control transcripts (RNAs 3000-3847 and 5418-6296) correspond to parts of the FMDV coding region or to the 5'UTR of normal eukaryotic mRNAs (hemoglobinase [14] and cathepsin B [7] of *S. mansoni*).

et al. (22). A ribosomal salt wash fraction was prepared as described above.

Cytoplasmic extracts from BHK and HeLa cells were prepared as follows. Approximately 10^8 confluent cells were scraped from culture dishes, pelleted, resuspended in 1 volume of buffer (22), and homogenized as described previously (4).

UV cross-linking. UV cross-linking was performed essentially as described by Pelletier and Sonenberg (23), with a few modifications. Ten nanograms of labeled RNA was incubated for 10 min at 25°C with 25 μg of protein extract (unless otherwise indicated) in a 30-μl total volume of binding buffer containing 250 μM GTP, 250 μM ATP, and 2.5 μg of yeast tRNA, but no monovalent cations (unless otherwise indicated). For competition assays, 0.1 or 1 μg unlabeled RNA was added in binding buffer. The addition of more unspecific competitor RNA or the use of different RNA species (tRNA from *Escherichia coli* or bovine rRNA) did not influence the specificity of the results. Samples were irradiated with 254-nm UV light for 1 h at 4°C with a 6-W UVP Inc. UVGL-55 Mineralight lamp. After irradiation, the RNA was digested with 20 μg of RNase A for 30 min at 37°C, the proteins were separated by electrophoresis on 10% sodium dodecyl sulfate (SDS)-polyacrylamide gels (17), and the protein-RNA complexes were visualized by autoradiography. Except for slight differences in the background pattern of unspecific protein bands, which were due mainly to the quality of the source of labeled RNA used, the results of this assay were highly reproducible.

RNA footprinting. To synthesize 5'-end-labeled RNA, we made use of the fact that all SP6 transcribed RNAs start with a guanosine nucleotide. SP6 transcription in the presence of [γ-^{32}P]GTP led to specifically 5' end labeled RNA. The transcription reaction was performed as described above, but in the presence of 6 μM [γ-^{32}P]GTP (>2,000 Ci/mmol; Amersham), 500 μM each ATP, CTP, and UTP, and 300 U of SP6 RNA polymerase per ml for 1 h at 40°C. For the chase, the GTP concentration was increased to 500 μM, and the sample was incubated for another 5 min at 40°C after addition of 100 U of SP6 RNA polymerase per ml. The reaction was stopped by phenol extraction, and labeled RNA was separated from free nucleotides by gel filtration on Sephadex G-100 (Pharmacia) and ethanol precipitation.

3' end labeling of RNA was performed with [^{32}P]Cp (Amersham) and T4 RNA ligase (New England Biolabs) by the method of Siegel and Walter (29).

For the preparation of RNA footprints, 5'- or 3'-end-labeled RNAs (10^4 to 10^5 cpm) were incubated for 10 min at 25°C and then for 10 min at 0°C without or with 10 to 20 μg of protein extract and 40 U of RNasin in a total volume of 40 μl of 20 mM Tris hydrochloride, 80 mM potassium acetate, 2 mM magnesium acetate, and 6 mM β-mercaptoethanol (pH 7.8). For partial digestion of the RNA, samples were incubated with 0.1 to 1 U of nuclease P1 (Boehringer Mannheim)

or 0.1 to 1 U of RNase V1 (Pharmacia) for 5 to 10 min at 25°C. Reactions were stopped by phenol and chloroform extraction and analyzed on 8% polyacrylamide gels containing 7 M urea.

RESULTS

A 57-kDa protein binds to two distinct sites in the 5′UTR of FMDV. We have recently shown that a 57-kDa protein from rabbit reticulocyte extracts can be specifically cross-linked to the 450-nt translation control region of FMDV by UV irradiation of a protein-RNA complex (18). To localize the binding site more precisely, RNA subfragments from that region were derived from plasmids pSP449 and pSP450, which initiate at two different sites at the 5′ border of the region (positions 362 and 399, respectively; Fig. 1A) and used in the cross-linking assay. As shown in Fig. 1B, a p57 complex can be observed with all RNA fragments starting at position 362, even those with very short sequences (RNAs 362-434 and 362-527). However, the fragment from position 362 to 831 corresponding to the complete translation initiation site leads to a stronger signal (RNA 362-831). If transcription initiates 37 nt further downstream at position 399, p57 does not bind to the short RNA fragments of the anterior part of this region (RNAs 399-434 and 399-527); if the 5′ shortened RNA reaches up to the start codon (RNA 399-831), a protein-RNA complex is formed again. These findings suggest the presence of two p57 binding sites, one at the 5′ end and another in the 3′ part of the IRES. We have localized the second binding site on the short RNA fragment 742-831, containing 62 nt upstream from the translation start site (Fig. 1B [18]). A short RNA fragment (nt 742 to 802) not containing the AUG codon binds p57 with the same affinity as does RNA fragment 742-831 (data not shown), indicating that binding of p57 to the 3′ site is independent of the presence of the start codon.

The central part of the IRES (RNA 399-742) does not bind p57. The p57 complex was observed if parts of the middle region were deleted (RNAs Δ519-559 and Δ581-672). In comparison with the complete sequence (RNA 362-831), binding of p57 to the deleted RNAs is weaker, suggesting a helper effect of the central sequence. Control transcripts corresponding to parts of the coding region of FMDV (RNAs 3000-3847 and 5416-6296) and the 5′UTR of a normal eukaryotic mRNA (cathepsin B of *Schistosoma mansoni*) do not react with p57. Unexpectedly, interaction of p57 with the mRNA of hemoglobinase from *S. mansoni* was observed.

Competition of p57 binding and effect of ion concentration on complex formation. To demonstrate binding of a single 57-kDa protein species to distinct sites, formation of a complex with both the 5′ and 3′ binding sites was analyzed in competition assays (Fig. 2A). A 10-fold excess of homologous unlabeled RNA 362-434 reduced binding of p57 to the labeled 5′ site markedly. Competition was nearly complete with a 100-fold excess of RNA 362-434. The same degree of competition was obtained with a 100-fold excess of RNA specific for the second binding site (RNA 742-831). Similarly, binding of p57 to the 3′ site (RNA 742-831) was efficiently competed for by a 100-fold excess of unlabeled RNA containing the 5′ binding site (RNA 362-434) or the 3′ binding site (RNA 742-831). An RNA fragment (399-434) containing neither the 5′ binding site nor the 3′ binding site was unable to compete for the p57 complex.

Additional proteins, predominantly a 110-kDa species, seem to bind specifically to the short RNA fragment 742-831, since they are competed for with an excess of homologous but not heterologous RNA. Most of this 110-kDa protein is found not in the ribosomal salt wash fraction but in the postribosomal supernatant. However, binding of this protein was not observed with the longer RNA 362-831. Thus, it remains to be clarified whether the long RNA cannot adopt the correct conformation to bind the 110-kDa protein or whether the short RNA fragment binds the protein artificially.

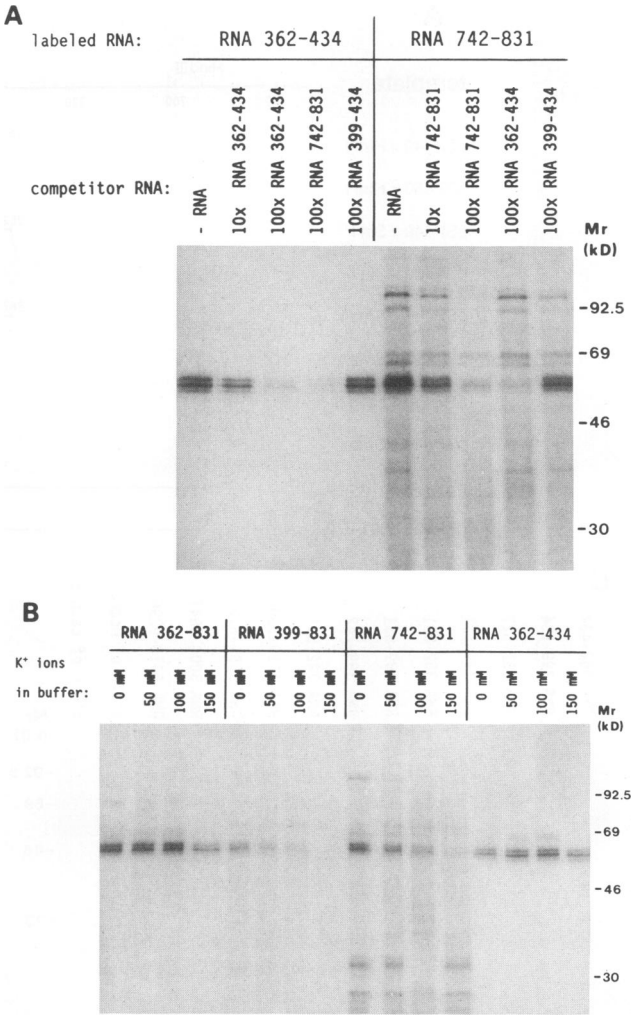

FIG. 2. Binding of p57 under different conditions. (A) Cross-competition of the two p57 binding sites, determined by UV cross-linking of the ribosomal salt wash fraction from rabbit reticulocytes with labeled RNA 362-434 or RNA 742-831 in the presence or absence of different amounts of unlabeled competitor RNA, as indicated. (B) UV cross-linking of p57 from rabbit reticulocytes to FMDV RNA fragments RNA 362-831, RNA 399-831, RNA 742-831, and RNA 362-434 in the presence of different potassium acetate concentrations, as indicated. The final KCl concentration in each reaction was 30 mM.

UV cross-linking of p57 to RNA fragments was analyzed in the presence of different salt concentrations (Fig. 2B). Binding of p57 to the entire translation control region (RNA 362-831) was similar at 30, 80, and 130 mM potassium, whereas a concentration of 180 mM potassium markedly decreased the strength of complex (the potassium ion concentration given in Fig. 2B had to be increased by 30 mM KCl because of the ribosomal salt wash fraction). Binding to

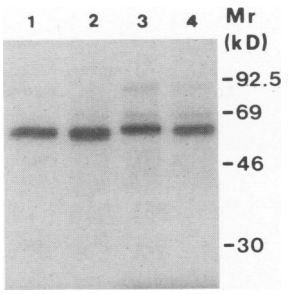

FIG. 3. UV cross-linking of proteins from cell extracts of different mammalian species to FMDV RNA 362-831. Total protein of the ribosomal salt wash fraction of rabbit reticulocytes (lane 1) and rat liver (lane 2) (15 μg each), 15 μg of total protein of a HeLa cell extract (lane 3), and 7 μg of total protein of a BHK cell extract (lane 4) were used.

the 3′ site (RNA 399-831 or 742-831) was highest in the absence of potassium acetate, was decreased by the addition of 50 and 100 mM potassium acetate, and was nearly abolished with 150 mM potassium acetate. In contrast, for p57 binding to the 5′ site (RNA 362-434), a concentration of 50 to 100 mM potassium acetate was optimal.

p57 is not limited to rabbit reticulocytes. To determine the occurrence of p57 in cells other than reticulocytes, we tested extracts from different tissues and cell lines from various species in UV cross-linking experiments with RNA 362-831 (Fig. 3). Complexes similar to those obtained with reticulocyte extracts were observed with a salt wash fraction from rat liver ribosomes, with a cytoplasmic HeLa extract, and with a cytoplasmic BHK cell extract, which suggests that p57 is a ubiquitous protein. Interestingly, the upper band of the p57 doublet is more intensive with the (total) extracts from BHK and HeLa cells. Possibly, a modified form of p57 corresponding to the upper band is not associated with ribosomes, as this band is not recognized in a ribosome salt wash of BHK cells (data not shown). Similar to the protein from rabbit reticulocytes, p57 from these different cell extracts is able to bind independently to the 5′ and 3′ ends of the IRES (data not shown).

p57 binds to the RNA of EMCV and poliovirus. Recently, Jang and Wimmer (13) demonstrated binding of a rabbit reticulocyte protein with a molecular size of 57 kDa to the 5′UTR of EMCV. To test whether the FMDV-specific 57-kDa protein would also bind to EMCV RNA and to poliovirus RNA, we performed cross linking experiments with in vitro-synthesized RNAs containing the 5′UTRs of these two viruses (Fig. 4). Incubation of the rabbit reticulocyte ribosomal salt wash fraction with EMCV RNA (lane 2) resulted in a signal comparable to that for FMDV RNA (lane 1), whereas with the same amount of poliovirus RNA, a weaker 57-kDa band was observed (lane 5). Several additional bands were observed with EMCV and poliovirus RNAs, which could indicate the participation of other factors in the translation initiation of these two viruses. However, they may also be due to technical factors, since the corresponding RNAs had to be synthesized under different in vitro conditions (see Materials and Methods).

To test whether the 5′UTR of FMDV would bind the same protein as did the EMCV and poliovirus RNAs, an excess of unlabeled FMDV RNA was used to compete for binding of p57 to the RNAs from EMCV and poliovirus. Formation of the complex with EMCV RNA was strongly reduced with a 10-fold excess of FMDV RNA (Fig. 4, lane 3) and abolished

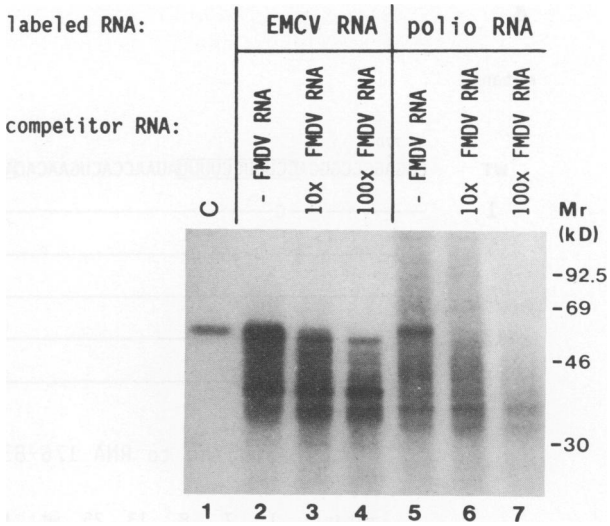

FIG. 4. UV cross-linking of proteins from the ribosomal salt wash fraction of rabbit reticulocytes to the 5′UTR of other picornaviruses. The specificity of p57 binding to 5′UTR of EMCV RNA (nt 260 to 837 [12]) and poliovirus RNA (nt 1 to 750 [15]) was tested by competition with FMDV RNA 362-831. The molar excess of competitor RNA is indicated. Lane C, complex with FMDV RNA 362-831 as a control.

with a 100-fold excess (lane 4), whereas binding to poliovirus RNA was fully competed for with a 10-fold excess of FMDV RNA (lanes 6 and 7), indicating that the same p57 species interacts with the 5′UTRs from these three picornaviruses.

Effect of single base exchanges in a pyrimidine-rich sequence on binding of p57. A sequence of 9 to 11 pyrimidine nucleotides precedes the two translation initiation codons of all FMDV strains, except for the second initiation site of type SAT3 (28). Recently we have shown that single base exchanges in the pyrimidine-rich sequence upstream of the first translation start site interfere strongly with the translation efficiency (16). The affinity of p57 for the RNAs of such mutants (listed in Fig. 5A) is not significantly affected if a long segment of the 5′UTR (RNA 176-831) is used in the binding assays (Fig. 5B). However, if the 5′ end of the mutated RNAs is deleted up to position 742, thus limiting the interaction of p57 to the 3′ binding site, the amount of complexed p57 parallels the translation efficiencies of the mutants (Fig. 5C). Single pyrimidine exchanges, which reduced the translation efficiency to levels 50 and 15% of the wild-type (wt) level (mutants 1 and 13), led to 80 and 40% binding of p57 to the corresponding 5′ shortened RNAs (Fig. 5A). Exchange of two or four nucleotides within the pyrimidine sequence, reducing the translation rate to levels 12 and 5%, respectively, of the wt level (mutants 25 and 7), decreased p57 binding to 25 and 13%.

Footprinting of cellular factors on the 5′UTR RNA. To analyze interactions of further cellular factors with the IRES of FMDV, we determined the RNase-sensitive sites within the entire region in the presence and absence of different fractions from reticulocyte extracts. The experiments were carried out with 5′- and 3′-end-labeled RNAs in separate experiments to resolve the complete region (positions 362 to 831). Three different fractions from purified rabbit reticulocyte ribosomes were tested: complete ribosomes, the 0.5 M ribosomal salt wash fraction, and ribosomes after the salt wash. The results for footprinting of the 5′-end-labeled RNA

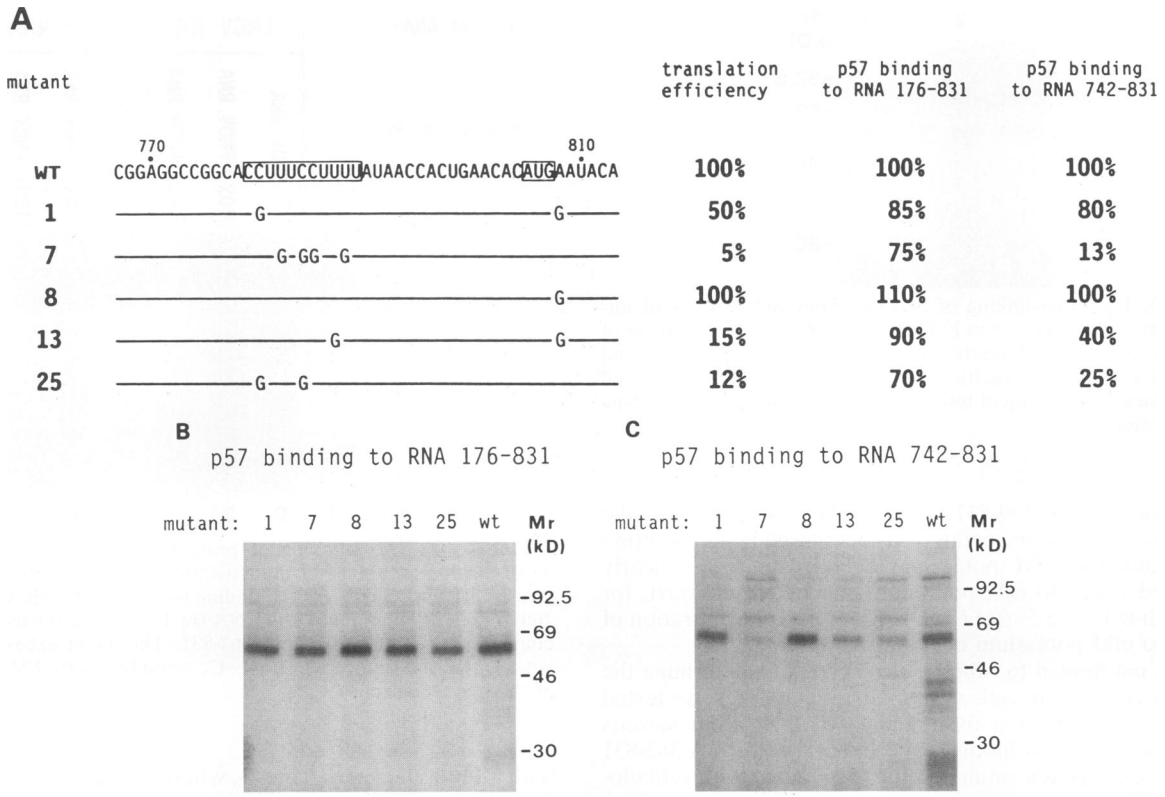

FIG. 5. Effect of single base exchanges near the translation start site on p57 binding. (A) Nucleotide sequence of FMDV RNA near the translation start site. The pyrimidine region and the start codon are boxed. For the individual mutant RNAs (no. 1 to 25), only nucleotides differing from the wt sequence are shown. The translation efficiency in rabbit reticulocyte lysates relative to wt RNA (16) is given on the right. Also shown are binding efficiencies of p57 to RNAs 176-831 and 742-831, as determined from the autoradiographs shown in panels B and C, respectively. The level of UV cross-linking was determined by scanning autoradiograms with a Hirschmann Elscript 400 scanner. The background pattern of nonspecific protein bands with the wt fragment 742-831 in the rightmost lane of panel C is exceptionally high and not representative (compare UV cross-linking with this fragment in Fig. 1B, 2A, and 2B).

are shown in Fig. 6. The ribosomal salt wash fraction as well as the unwashed ribosomes protected several nucleotides against digestion with the single-strand-specific nuclease P1 (compare lanes RSW and ribosomes with lane − protein). The nucleotides at positions 405/406, 413/415, 492, 511, and 575 were protected by both fractions. Position 522 was protected only by the ribosomal salt wash fraction. In contrast, washed ribosomes did not protect the RNA (lane salt washed rib.). Interestingly, no protection against the double-strand-specific RNase V1 was observed in any case. In contrast, the presence of unwashed ribosomes and of the ribosomal wash fraction appeared to enhance RNase sensitivity in several positions.

Footprint experiments with 3′-end-labeled RNA confirmed the results obtained with the 5′-end-labeled RNA (data not shown). Protection of nt 492, 511, and 575 against P1 digestion in the presence of both the ribosomal salt wash fraction and the complete ribosomes was clearly observed. In addition, an RNase-resistant triplet not resolved on the footprint in Fig. 6 was observed in positions 764 to 766. These nucleotides are localized close to the pyrimidine-rich region mentioned above and may therefore represent part of the putative 3′ binding site of p57 (data not shown).

In control incubations in the absence of RNase, no significant differences were observed in the background patterns of labeled RNA bands with or without the protein extracts, indicating the absence of endogenous RNase activity. The bands observed in these lanes correspond to incomplete transcription of the template DNA and are probably due to the high degree of secondary structure in this region.

DISCUSSION

p57 binds to two sites within the 5′UTR of FMDV RNA. In this report, we demonstrate that a cellular 57-kDa protein interacts with two distinct sites at the 5′ and 3′ ends of the IRES of FMDV RNA. Contacts of p57 with the middle part of the IRES were not identified, but the intact control region binds the protein much more strongly, suggesting a supplementary effect of the central RNA segment on complex formation. By cross-competition experiments, it was shown that a single p57 species binds to the two sites. The equal competition of the two corresponding RNA fragments indicates a similar affinity of p57 for both sites.

The two binding sites in the 5′UTR of FMDV are more than 300 nt apart, but the secondary structure models of the IRES of the cardiovirus-aphthovirus group (25) suggest that these sites may be located close together such that both of them could be in contact with one protein (Fig. 7). In this case, the protein would have to possess two distinct RNA binding domains which might have different specificities. Alternatively, both binding elements could be complexed with different p57 molecules, and the two ends of the IRES may be held together via p57 dimerization that might not

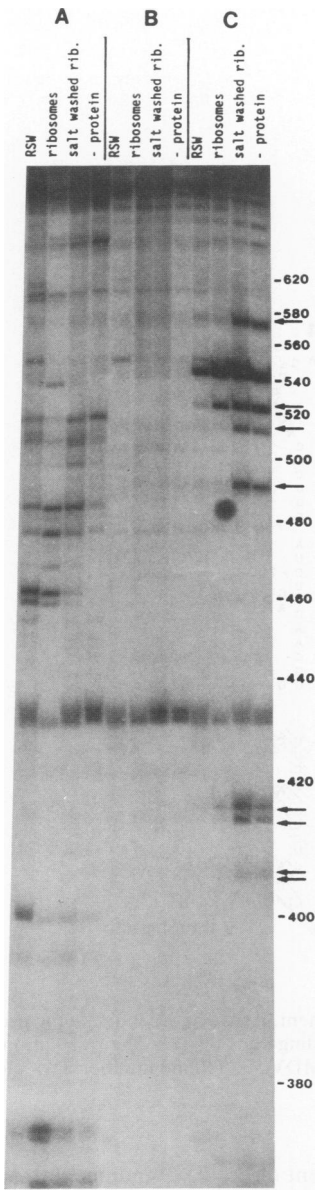

FIG. 6. RNA footprint of FMDV RNA 362-831 with different fractions of rabbit reticulocyte lysate. Shown is partial digestion of 5'-end-labeled FMDV RNA with double-strand-specific RNase V1 (A) or single-strand-specific nuclease P1 (C) in the presence of 0.5 M ribosomal salt wash fraction (RSW), complete ribosomes (ribosomes), or ribosomes after the salt wash (salt washed rib.) or without protein (− protein), as indicated. (B) Control incubations in the absence of RNase. Footprinting reactions were carried out as described in Materials and Methods. Numbers refer to positions on the FMDV RNA (8). Arrows point to protected positions.

only stabilize the tertiary structure but also allow the entering ribosomes to "jump" over most of the extended primary sequence. In that case, one would expect identical or similar sequences and structures in the limits of the experimentally determined p57 binding regions (positions 362 to 434 and 742 to 831). The only direct homology consists of a conserved UUUC motif which represents the single-stranded loop structure in the 5' binding site and is embedded into the pyrimidine stretch of the 3' site of all FMDV strains (28). This short sequence cannot represent the complete recognition signal, since it occurs also in other positions which do not interact with p57. However, as discussed below, it probably represents a constituent of the p57 binding site.

In footprint experiments (Fig. 6), we identified RNase-protected nucleotides in the IRES of FMDV which may result from binding of p57 and probably some other factors to the RNA. These protected positions are indicated in a secondary structure model of the IRES in Fig. 7. Protection was observed only with the single-strand-specific nuclease P1. Therefore, it seems that the RNA-binding factors bind mainly to single-stranded regions. The protected nucleotides (arrowheads in Fig. 7) on stem-loop structures 2 and 5 are probably part of the p57 binding sites, since they are located within the limits of the minimal RNA fragments determined so far. Other protected sites are localized on large stem-loop structure 3, but these sites may not be in contact with p57, since the corresponding RNA fragment (RNA 399-742) does not bind p57 upon UV irradiation. Nevertheless, the large central stem-loop structure is an essential element of the IRES, and deletions in this structure result in a strong decrease of the translation efficiency of FMDV (16).

Binding of p57 to other picornavirus RNAs. With respect to the nucleotide sequence of the 5'UTR, the picornaviruses can be divided in two groups, one consisting of the genera *Cardiovirus* and *Aphthovirus* and the other consisting of the genera *Enterovirus* and *Rhinovirus* (25, 26, 27). Although these regions are functionally equivalent, there is very little similarity in primary and predicted secondary structure between the two viral groups.

A 57-kDa protein binding to the 5'UTR of EMCV RNA was described by Jang and Wimmer (13) and Borovjagin et al. (1). This protein is identical with p57, since the complex with EMCV RNA can be competed for with FMDV RNA. Only one p57 binding site has been observed for EMCV RNA, although the 5'UTRs of FMDV and EMCV appear to be very similar on the basis of computer-aided secondary structure predictions and biochemical studies (25). The EMCV-specific site corresponds to the 5' binding site of FMDV (RNA 362-434) and seems to be represented by a conserved hairpin (no. 2) in the predicted secondary structure model of the IRES of the cardiovirus-aphthovirus group (Fig. 7). Complex formation is abolished if the RNA initiates in the middle of the stem-loop structure (position 399) or if the stem structure is destabilized by site-directed mutagenesis as shown for EMCV (13) but is restored by compensatory mutations. Whereas the primary sequence of the loop is conserved between the different virus species, only the length of the stem region, not its nucleotide sequence, is conserved. The fact that no binding of p57 to the 3' end of the IRES has been observed for EMCV may be due to differences in the nucleotide sequence of that region between EMCV and FMDV. Alternatively, this finding could be due to the fact that these authors used different binding conditions. As shown above, binding of p57 to this site in FMDV depends on specific salt concentrations. Whereas the complex at the 5' binding site is enhanced at 50 to 100 mM potassium acetate, optimal binding to the isolated 3' site was observed in the absence of potassium acetate (Fig. 2B).

p57 binds also to the 5'UTR of poliovirus, but the complex is weaker and can be competed for by a small excess of FMDV RNA. One reason for the weaker binding of p57 to poliovirus RNA might be that the affinity of this protein for the RNA is influenced by the interaction with other cellular factors that participate in the poliovirus-specific initiation complex but are not present in reticulocytes. It is well

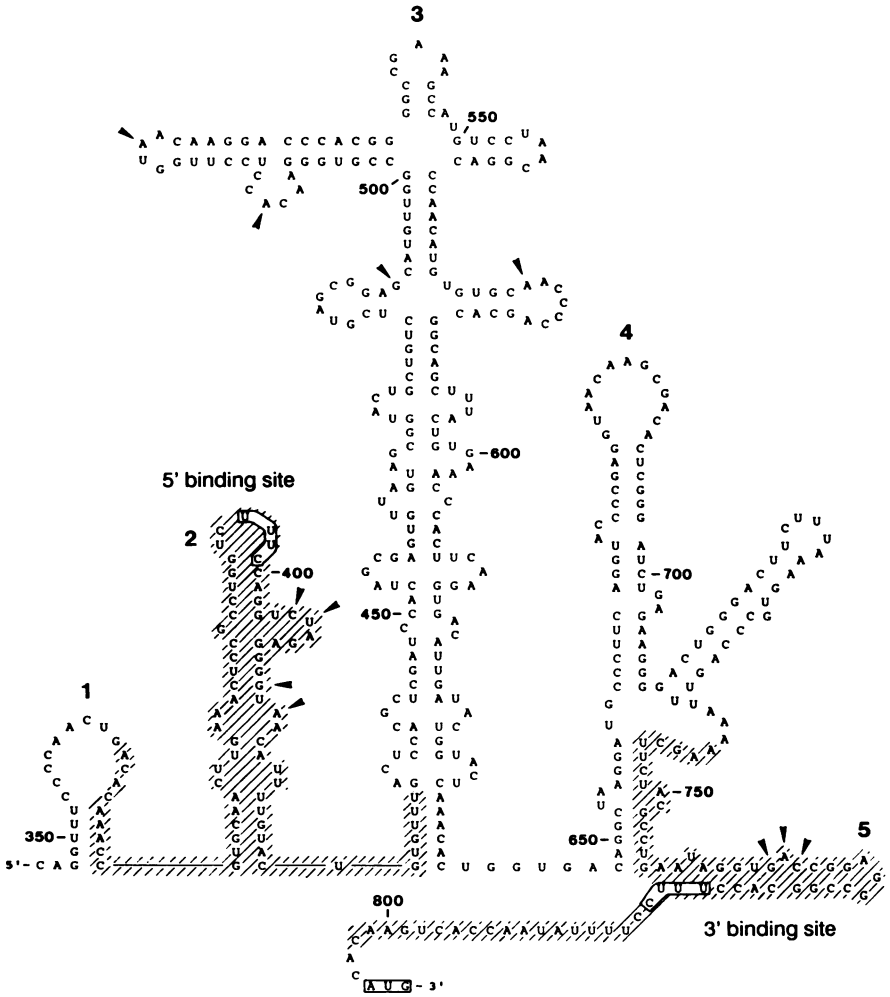

FIG. 7. Secondary structure of the 5'UTR segment of FMDV containing the IRES element. Arrowheads indicate the protected nucleotides identified by RNA footprinting in Fig. 6. Striped regions correspond to the 5' and 3' binding sites of p57. The translation start site at the 3' end of the RNA and the UUUC motifs are boxed. The secondary structure model of the FMDV 5'UTR and numbering of stem-loops predicted by Pilipenko et al. (25) are used.

known that poliovirus RNA is efficiently translated in reticulocyte lysates only upon supplementation with HeLa cell extract (5). A 52-kDa protein identified in the postribosomal fraction of HeLa cells (19) and a membrane-associated 50-kDa protein of HeLa cells (21) interacting with specific regions in the poliovirus IRES are possible candidates for such essential factors.

We have found p57 not only in rabbit reticulocytes but also in rat liver, HeLa, and BHK cells (Fig. 4). p57 of all of these extracts is able to bind the RNAs of FMDV, EMCV, and poliovirus (data not shown). Therefore, p57 may represent a highly conserved, ubiquitous protein.

What is the structure of the p57 binding site? The UUUC motif is the only conserved sequence between the different p57 binding sites and occurs in the corresponding pyrimidine tracts of all FMDV strains (28). Notably, exchanges within this pyrimidine-rich sequence affected the translation efficiency much more strongly than do mutations elsewhere in the surrounding nucleotides (16). In addition, single pyrimidine-purine exchanges in this motif interfere with the complex formation between p57 and the 5' binding site (17a). It is therefore very probable that the UUUC sequence is an essential element of the p57 binding site. A double-stranded structure as in case of the 5' binding site (13) cannot be observed for the 3' binding site. However, the pyrimidine stretch alone, including the UUUC motif, does not meet all conditions for specific binding, since the RNA in front of the second translation start codon of FMDV O1K, which also contains such a pyrimidine sequence, does not bind p57 (17a, 28). If we investigated the mutants of the pyrimidine-rich sequence in the context of the complete IRES for p57 binding, slightly less binding activity than for the wt RNA (less than a factor of 2) was observed. However, complex formation with the mutagenized 3' binding sites alone was strongly affected. This correlation between the translation efficiency and binding of p57 to the 3' binding site suggests that p57 is essential for the internal translation initiation of FMDV RNA. An analogous pyrimidine-rich sequence upstream from the polyprotein coding region was recently shown to be essential for efficient translation initiation of EMCV (13). These authors postulate the interaction of an unknown cellular factor X with this sequence, but in view of the structural and functional homology, it is conceivable, although not yet demonstrated, that p57 binds to both sites.

From the work of Jang and Wimmer (13), it also seems that the number of pyrimidine residues and the correct distance from the translational start codon are crucial.

Different fragments of the coding and noncoding parts of the FMDV genome, including those containing UUUC sequences, and some eukaryotic mRNAs used as controls (in vitro-synthesized mRNAs of cathepsin B and a fatty acid-binding protein of *S. mansoni* [not shown]) did not bind p57. However, another mRNA of *S. mansoni* (coding for hemoglobinase) formed a specific complex with the protein. We could limit the binding site to the 5′ part of the mRNA, which consists of 32 untranslated nt in front of the start codon and approximately 100 nt of the coding region. There is a pyrimidine-rich sequence of 14 nt (interrupted by a single adenosine residue) downstream from the translation start site (14). It is highly unlikely that the translation starts at an internal site, since this mRNA is more efficiently translated if an m^7-cap nucleotide is added to the 5′ end. Rather, we think that the mRNA sequence mimics a p57 binding site by chance. We can take this sequence (which again carries a UUUC motif) as another example which may help to unravel the puzzling structural features of a p57-specific binding site.

The obviously crucial role of pyrimidine residues in the p57 RNA interaction resembles that of a recently identified nuclear-associated 62-kDa protein which binds to the polypyrimidine tract near the 3′ splice site of introns (9). Not a specific primary nucleotide sequence but rather the total number of pyrimidine nucleotides seems to be important for binding of that protein. Interestingly, the authors also observed that this 62-kDa protein was resolved into a double band or a triplet of bands after UV cross-linking, which again parallels the observation for p57 (Fig. 2). The chemical nature of this variation is unclear.

Future work will show whether one or more additional proteins play a crucial role in this extraordinary recognition complex for internal translation initiation.

ACKNOWLEDGMENTS

We thank Hans-Georg Kräusslich for critical reading of the manuscript.

This work was supported by grant BCT 381-5 from the Bundesministerium für Forschung und Technologie. N.L. is the recipient of a Landesgraduiertenförderungsgesetz, Baden-Württemberg, stipend.

REFERENCES

1. **Borovjagin, A. V., A. G. Evstafieva, T. Y. Ugarova, and I. N. Shatsky.** 1990. A factor that specifically binds to the 5′-untranslated region of encephalomyocarditis virus RNA. FEBS Lett. **261**:237–240.
2. **Clemens, M. J.** 1984. Translation of eukaryotic messenger RNA in cell-free extracts, p. 231–270. *In* B. D. Hames and S. J. Higgins (ed.), Transcription and translation—1984. IRL Press Ltd., Oxford.
3. **del Angel, R. M., A. G. Papavassiliou, C. Fernández-Tomás, S. J. Silverstein, and V. R. Racaniello.** 1989. Cell proteins bind to multiple sites within the 5′ untranslated region of poliovirus RNA. Proc. Natl. Acad. Sci. USA **86**:8299–8303.
4. **Dissous, C., C. Verwaerde, C. Lempereur, and J. Krembel.** 1978. Free and membrane-bound polysomes from rat liver. Eur. J. Biochem. **83**:5–15.
5. **Dorner, A. J., B. L. Semler, R. J. Jackson, R. Hanecak, E. Duprey, and E. Wimmer.** 1984. In vitro translation of poliovirus RNA: utilization of internal initiation sites in reticulocyte lysate. J. Virol. **50**:507–514.
6. **Falk, M. M., P. R. Grigera, I. E. Bergmann, A. Zibert, G. Multhaup, and E. Beck.** 1990. Foot-and-mouth disease virus protease 3C induces specific proteolytic cleavage of host cell histone H3. J. Virol. **64**:748–756.
7. **Felleisen, R., and M.-Q. Klinkert.** 1990. In vitro translation and processing of cathepsin B of Schistosoma mansoni. EMBO J. **9**:371–377.
8. **Forss, S., K. Strebel, E. Beck, and H. Schaller.** 1984. Nucleotide sequence and genome organization of foot-and-mouth disease virus. Nucleic Acids Res. **12**:6587–6601.
9. **Garía-Blanco, M. A., S. F. Jamison, and P. A. Sharp.** 1989. Identification and purification of a 62,000-dalton protein that binds specifically to the polypyrimidine tract of introns. Genes Dev. **3**:1874–1886.
10. **Jackson, R. J., M. T. Howell, and A. Kaminski.** 1990. The novel mechanism of initiation of picornavirus RNA translation. Trends Biochem. Sci. **15**:477–483.
11. **Jang, S. K., M. V. Davies, R. J. Kaufman, and E. Wimmer.** 1989. Initiation of protein synthesis by internal entry of ribosomes into the 5′ nontranslated region of encephalomyocarditis virus RNA in vivo. J. Virol. **63**:1651–1660.
12. **Jang, S. K., H.-G. Kräusslich, M. J. H. Nicklin, G. M. Duke, A. C. Palmenberg, and E. Wimmer.** 1988. A segment of the 5′ nontranslated region of encephalomyocarditis virus RNA directs internal entry of ribosomes during in vitro translation. J. Virol. **62**:2636–2643.
13. **Jang, S. K., and E. Wimmer.** 1990. Cap-independent translation of encephalomyocarditis virus RNA: structural elements of the internal ribosomal entry site and involvement of a cellular 57-kD RNA-binding protein. Genes Dev. **4**:1560–1572.
14. **Klinkert, M.-Q., R. Felleisen, G. Link, A. Ruppel, and E. Beck.** 1989. Primary structures of Sm31/32 diagnostic proteins of Schistosoma mansoni and their identification as proteases. Mol. Biochem. Parasitol. **33**:113–122.
15. **Kräusslich, H.-G., C. Hölscher, Q. Reuer, J. Harber, and E. Wimmer.** 1990. Myristoylation of the poliovirus polyprotein is required for proteolytic processing of the capsid and for viral infectivity. J. Virol. **64**:2433–2436.
16. **Kühn, R., N. Luz, and E. Beck.** 1990. Functional analysis of the internal translation initiation site of foot-and-mouth disease virus. J. Virol. **64**:4625–4631.
17. **Laemmli, U. K.** 1970. Cleavage of structural proteins during the assembly of the head of bacteriophage T4. Nature (London) **227**:680–685.

17a. **Luz, N.** Unpublished data.

18. **Luz, N., and E. Beck.** 1990. A cellular 57 kDa protein binds to two regions of the internal translation initiation site of foot-and-mouth disease virus. FEBS Lett. **269**:311–314.
19. **Meerovitch, K., J. Pelletier, and N. Sonenberg.** 1989. A cellular protein that binds to the 5′-noncoding region of poliovirus RNA: implications for internal translation initiation. Genes Dev. **3**:1026–1034.
20. **Melton, D. A., P. A. Krieg, M. R. Rebagliati, T. Maniatis, K. Zinn, and M. R. Green.** 1984. Efficient in vitro synthesis of biologically active RNA and RNA hybridization probes from plasmids containing a bacteriophage SP6 promoter. Nucleic Acids Res. **12**:7035–7056.
21. **Najita, L., and P. Sarnow.** 1990. Oxidation-reduction sensitive interaction of a cellular 50-kDa protein with an RNA hairpin in the 5′ noncoding region of the poliovirus genome. Proc. Natl. Acad. Sci. USA **87**:5846–5850.
22. **Nygård, O., P. Westermann, and T. Hultin.** 1980. The use of rRNA-cellulose chromatography in the rapid isolation of homogeneous protein synthesis initiation factor eIF-2 from rat liver microsomes. Biochim. Biophys. Acta **608**:196–200.
23. **Pelletier, J., and N. Sonenberg.** 1985. Photochemical cross-linking of cap binding proteins to eucaryotic mRNAs: effect of mRNA 5′ secondary structure. Mol. Cell. Biol. **5**:3222–3230.
24. **Pelletier, J., and N. Sonenberg.** 1988. Internal initiation of translation of eukaryotic mRNA directed by a sequence derived from poliovirus RNA. Nature (London) **334**:320–325.
25. **Pilipenko, E. V., V. M. Blinov, B. K. Chernov, T. M. Dmitrieva, and V. I. Agol.** 1989. Conservation of the secondary structure elements of the 5′-untranslated region of cardio- and aphthovirus RNAs. Nucleic Acids Res. **17**:5701–5711.
26. **Pilipenko, E. V., V. M. Blinov, L. I. Romanova, A. N. Sinyakov, S. V. Maslova, and V. I. Agol.** 1989. Conserved structural

domains in the 5′-untranslated region of picornaviral genomes: an analysis of the segment controlling translation and neurovirulence. Virology **168**:201–209.

27. **Rivera, V. M., J. D. Welsh, and J. V. Maizel, Jr.** 1988. Comparative sequence analysis of the 5′ noncoding region of the enteroviruses and rhinoviruses. Virology **165**:42–50.
28. **Sangar, D. V., S. E. Newton, D. J. Rowlands, and B. E. Clarke.** 1987. All foot and mouth disease virus serotypes initiate protein synthesis at two separate AUGs. Nucleic Acids Res. **15**:3305–3315.
29. **Siegel, V., and P. Walter.** 1988. Binding sites of the 19-kDa and 68/72-kDa signal recognition particle (SRP) proteins on SRP RNA as determined by protein-RNA "footprinting." Proc. Natl. Acad. Sci. USA **85**:1801–1805.
30. **van der Werf, S., J. Bradley, E. Wimmer, F. W. Studier, and J. J. Dunn.** 1986. Synthesis of infectious poliovirus RNA by purified T7 RNA polymerase. Proc. Natl. Acad. Sci. USA **83**:2330–2334.
31. **Woodley, C. L., Y. C. Chen, and K. Gupta.** 1973. Purification and properties of peptide chain initiation factors from rabbit reticulocytes. Methods Enzymol. **30**:141–153.